ROPME/GC-15/3
Dist.: RESTRICTED

ROPME/IAEA 2011
RECONSTRUCTION OF OIL POLLUTION HISTORY IN THE ROPME SEA AREA

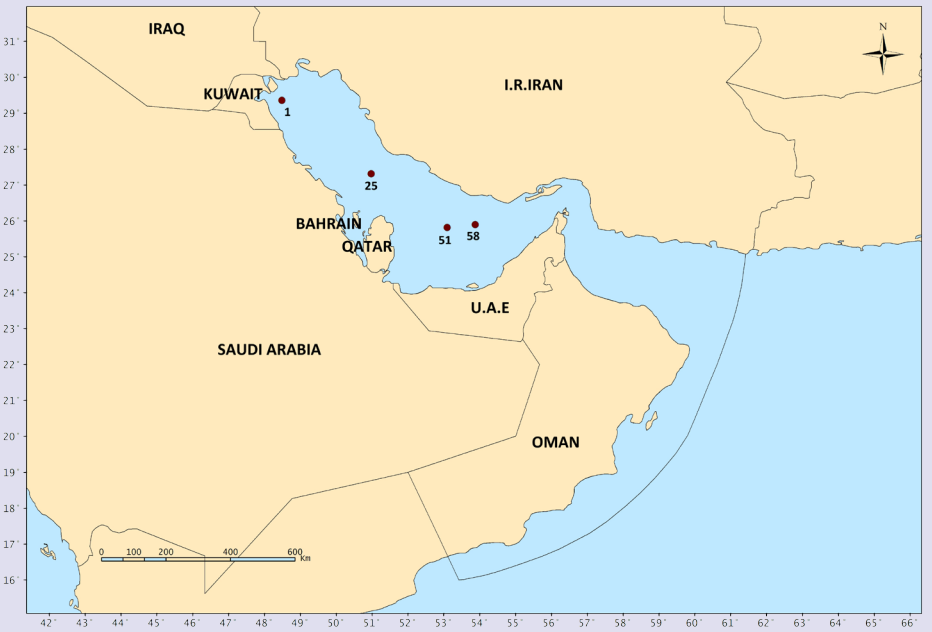

FINAL REPORT

Prepared by:

MESL/IAEA
Monaco, September 2012

For:

REGIONAL ORGANIZATION FOR THE PROTECTION OF THE MARINE ENVIRONMENT

The Regional Organization for the Protection of the
Marine Environment (ROPME)
P.O. Box 26388
13124 Safat
Kuwait

TABLE OF CONTENTS

ANNEX - I

LIST OF TABLE

LIST OF FIGURES

1. INTRODUCTION

This interpretation report is the follow up to the data report on reconstruction of oil pollution history undertaken by MESL/IAEA for ROPME on sediment cores prepared from four sampling stations in the ROPME Sea Area.

2. SAMPLING METHODOLOGY

The sampling stations, locations and the types of samples collected are given in the Table 1 and shown in Figure 1.

The samples were received by the MESL/IAEA already freeze-dried in small glass bottles.

Table 1. Sampling stations, locations and types of samples to reconstruct oil pollution history in RSA

ROPME Cruise 2006- Sediment GRAB				Group-2
STATION	1	25	51	58
DATE	9/3/2006	3/3/2006	22/2/2006	21/2/2006
Depth (m)	13.00	67.00	60.00	75.00
LATITUDE	29° 21.000'	27° 18.290'	25° 48.625'	25° 53.289'
LONGITUDE	48° 29.000'	50° 58.400'	53° 05.650'	53° 52.585'

NB: Availabl weight for each grab sediment sample is 30 g

ROPME Summer 2001 - Sediment CORE				Group-1
STATION	1	25	51	58
DATE	27/08/2001	21/08/2001	12/08/2001	10/08/2001
Depth (m)	13.87	66.51	57.96	75.51
LATITUDE	29° 20.510	27° 18.352	25° 47.800	25° 52.231
LONGITUDE	48° 33.135	50° 59.106	53° 06.180	053° 52.768

	Station 1		Station 25		Station 51		Station 58	
Total Sediment Core L (cm)	41.00		26.00		34.00		43.00	
	Section	(g)	Section	(g)	Section	(g)	Section	(g)
	1	10	1	13	1	14	1	13
	2	18	2	21	2	16	2	9
	3	20	3	21	3	17	3	13
	4	28	4	22	4	18	4	17
	5	23	5	22	5	19	5	16
	6	23	6	21	6	19	6	16
	7	25	7	14	7	21	7	12
	8	22	8	21	8	18	8	18
	9	28	9	25	9	17	9	21
	10	22	10	24	10	16	10	14
	11	29						

Notes: -Sections from 1 to 10 in each core of Cruise 2001 represent 1-cm thickness (gp-1)
- Sec.11 of Core-1 repesents the remainde sediment within the 31 cm deeper
-Sediment samples from Cruise 2006 represent the upper 5-cm depth of the grab (gp-2)
-Known rate of sedimentation in the RSA are ranging between 0.5 and 1.0 cm/yr which needs confirmtion

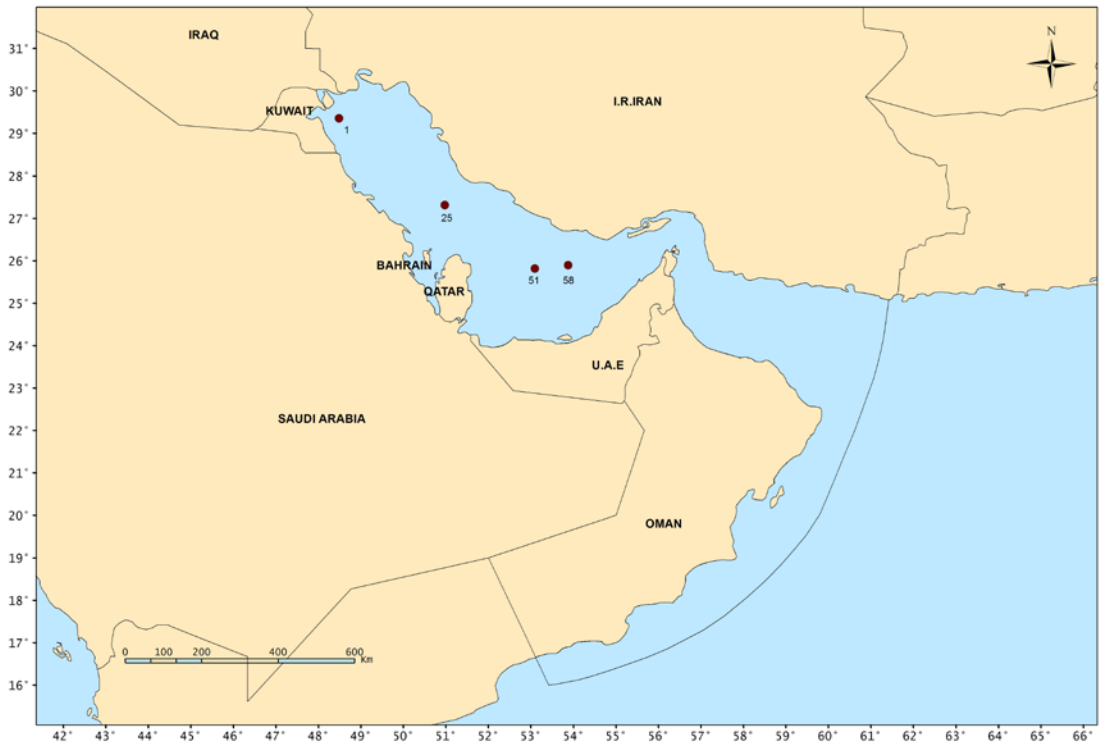

Figure 1. Map showing the sediment cores sampling stations.

3. ANALYTICAL PROCEDURES

The analytical protocols for measuring petroleum hydrocarbons are detailed in this section.

3.1. SEDIMENT SAMPLES

3.1.1. Sample pre-treatment and extraction

The freeze-dried samples were grinded and sieved through stainless steel sieves with mesh sizes of 250 µm. Sediments were then homogenized prior to extraction.

The extraction was realized with a microwave oven. Ten to 15 grams of freeze-dried sediment sample were put in the glass tube of the reactor with 40 ml of a mixture of hexane:dichloromethane (50:50). Internal standards were added, these standards are used for quantifying the overall recovery of the analytical procedures:

- *n*-C_{24}-d_{50} for the aliphatic hydrocarbon fraction; Friedeline as GC internal standard;
- Hexamethylbenzene for the unresolved compounds from the aromatic hydrocarbon fraction; Friedeline as GC internal standard;
- Naphthalene-d_8, Acenaphtene-d10, Phenanthrene-d10, Chrysene-d10, Perylene-d12 (aromatics) for the aromatic hydrocarbon fraction; Fluorene-d10, Benzo(a)pyrene-d12 as GC internal standard.

The operating conditions of the microwave oven were as follows:

- Power of the microwave: 1200 Watts;
- Temperature increased to 115°C in 10 minutes; Extraction maintained at 115°C for 20 minutes; and
- Cooling to ambient temperature within one hour.

After cooling down to room temperature, the solvent mixture was recovered in a 100 ml glass flask. The sediment was rinsed with 2 x 5 ml of a *n*-hexane:dichloromethane (1:1) solution using a vacuum pump.

A sulphur removal procedure was performed using activated elemental copper in order to avoid sulphur interference when using gas chromatography. Sulphur compounds are specially detected and can cause interference in the analysis of chlorinated hydrocarbons.

Extractable Organic Matter (EOM) was determined by evaporating a measured small volume of this extract on the pan of an electro-balance.

3.1.1.1. Clean-up and fractionation

The concentrated extract of about 1 ml was passed through a silica/cianopropyl SPE glass column of 6 ml. The first fraction containing aliphatic compounds is obtained by eluting with 4 ml of *n*-hexane. The second fraction containing PAHs is obtained by eluting with 5 ml of a *n-h*exane:dichloromethane (1:1) solution. Both fractions are concentrated to about 0.5 ml (prior to solvent change from n-hexane to isooctane) and analyzed by GC.

3.1.1.2. Quantification and quality control

3.1.1.2.1. Hydrocarbons

UVF procedure

Emission scans and synchronous excitation/emission scans were recorded to evaluate the relative fluorescence and to characterize the aromatic hydrocarbons in the samples. Standard response curves of fluorescence intensity versus concentration were generated for Kuwait crude (ROPME) oil and for the standard aromatic hydrocarbon: Chrysene. Samples were diluted in order to give a reading within the linear calibration range of the fluorometer. Conditions of the fluorometer were adjusted as follows:

1st Procedure

Excitation wavelength fixed: 310 nm

a) Single calibrated measurement: Emission wavelength at 360 nm;

b) Scan: Emission wavelength from 320 nm to 550 nm.

cGC-FID conditions used were as follows:

Both aliphatic and aromatic hydrocarbon fractions were analyzed using cGC-FID.

Gas Chromatograph	Agilent 7890
Detector	Flame Ionization Detector (FID)
Injection mode	Splitless
Carrier gas	Helium 1.2 ml min^{-1}
Column	HP-5 (crosslinked 5% Ph Me Silicone) 30 m x 0.25 mm i.d. x 0.25 μm film thickness
Injector temperature	270°C
Detector temperature	300°C
Oven temperature program	60°C initial for 1 min., 60°C to 290°C at 4°C min^{-1}, 290°C for 40 min.

cGC-MS conditions used were as follows:

The aromatic hydrocarbons were analyzed using selective ion monitoring (SIM) to enhance sensitivity.

Gas Chromatograph	Agilent 6890 N
Detector	MSD 5975
Injection mode	Splitless
Carrier gas	Helium 1.5 ml min^{-1}
Column	DB-XLBMSD 30 m x 0.25 mm i.d. x 0.25 µm film thickness
Injection specifications	inj. press.: 13 psi, Constant flow on 13 psi at 60°C, Temp. injector 270°C
Transfer line	280°C
Ion source	240°C
Analyzer	100°C
Oven temperature program	60°C initial, 60°C to 100°C at 10°C min^{-1}, 100°C to 285°C at 4°C min^{-1}, 285°C for 20 min.

Appropriate blanks were analyzed with each set of analyses and in addition, the certified reference material IAEA-159 (IAEA, sediment) was measured simultaneously. This sediment has certified concentrations of hydrocarbons.

3.1.2. Total organic carbon and carbonates

The contents of total carbon (TC) and total organic carbon (TOC) were determined by using a CHN analyzer (Carlo Erba model 1602). Approximately 10–40 mg of dry sediment was encapsulated into a Sn foil cup and introduced into a combustion furnace. Organic carbon was determined after treating the samples with concentrated H_3PO_4 to remove inorganic carbon. Concentration of total organic carbon is expressed as the percentage of total dry weight. Carbonate content was calculated by subtracting the TOC from the TC content. Quality control was realized by measuring TC and TOC levels in a Certified Reference Material (SMR 1941b), providing information value for TC (3.3%) and reference value for TOC (2.99% ±0.24). The measured mean value obtained for TC was 3.18% ±0.02 (n=4) and 2.37% ±0.24 (n=10) for TOC.

3.1.3. Grain size

3.1.3.1. Preparation of samples

The samples were sieved at 300 m. Two samples could not be prepared as not enough samples were left following other measurements: GR1-ST51-S9 and GR1-ST58-S2.

Preparation prior particle size analysis

Approximately an aliquot of 1 g (or less when not enough material was available) of sediment was put in a 10 ml tube. 5 ml of MilliQ water was added and tube was shaken in order to separate the silt particles properly. An equilibration period of about half an hour was used to assure that the sample was uniformly wet before analysis.

3.1.3.2. Particle size analysis

The particle size distribution was determined using a Malvern Instrument Mastersizer device. The principle of this device is that small particles cause incident light to be diffracted through a large angle whereas large particles will diffract incident light through a small angle. Particle size information is derived by deconvulation of the diffraction data obtained by the instrument.

3.1.3.3. Apparatus used

The MALVERN Mastersizer Micro v2.12 is designed to analyze particle size of silt sediments (<300 µm), particles need to stay in suspension during the measurement process (this device is not suited for the analysis of coarse sandy material).

3.1.3.4. Protocol used

The analysis of particles is achieved by slurring a sediment sample into a beaker containing 500 ml of water. The mixture is pumped through a cell which is interrogated by the instrument's laser beam. The particle size distribution is determined from the resulting diffraction pattern.

3.1.3.5. Results of grain size analysis

The size distribution in percentage for each sample is reported as:

% Sand = ∑ percentage of particulates between 300 µm and 63 µm
% Silts = ∑ percentage of particulates between 63 µm and 3.9 µm
% Clay = ∑ percentage of particulates below 3.9 µm
% Mud = ∑ % Clay and % Silt.

4. RESULTS AND DISCUSSIONS

The proposed construction of the sediment core for the study of the oil pollution reconstruction is given in the Figure 2.

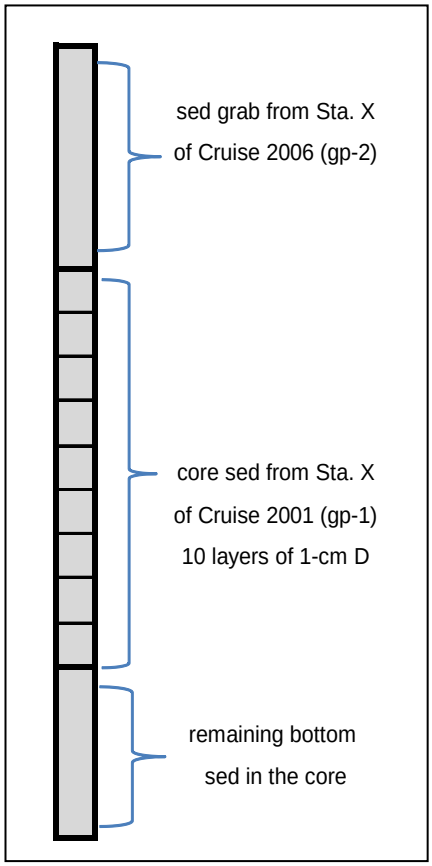

Figure 2. Construction sediment core for the study.

The concentrations of different classes of hydrocarbons, bulk parameters and diagnostic ratios for each sediment core are summarized in the Tables I.1, I.2, I.3 and I.4 from the Annex I.

The vertical distribution of total organic carbon (TOC) concentrations for each sediment core is illustrated in the Figure 3. The sediment core collected in station 1 is generally characterized by a relatively low content of TOC (0.4 to 0.9%), and most of the values fell under the value of 0.7%. The station 25 exhibited TOC concentrations relatively constant throughout the core (1 to 1.4%), except for the peak TOC concentration measured in the S8 (2.2%). Relatively higher and homogeneous TOC concentrations were measured in the

stations 51 and 58 with values ranging from 1.0 to 1.52% and 1.44 to 1.70%, respectively. As it was found in previous investigations in the same area, the lack of correlation between TOC and TPH content indicates that TOC cannot be used as an indicator of PH pollution in the RSA (de Mora *et al*., 2010).

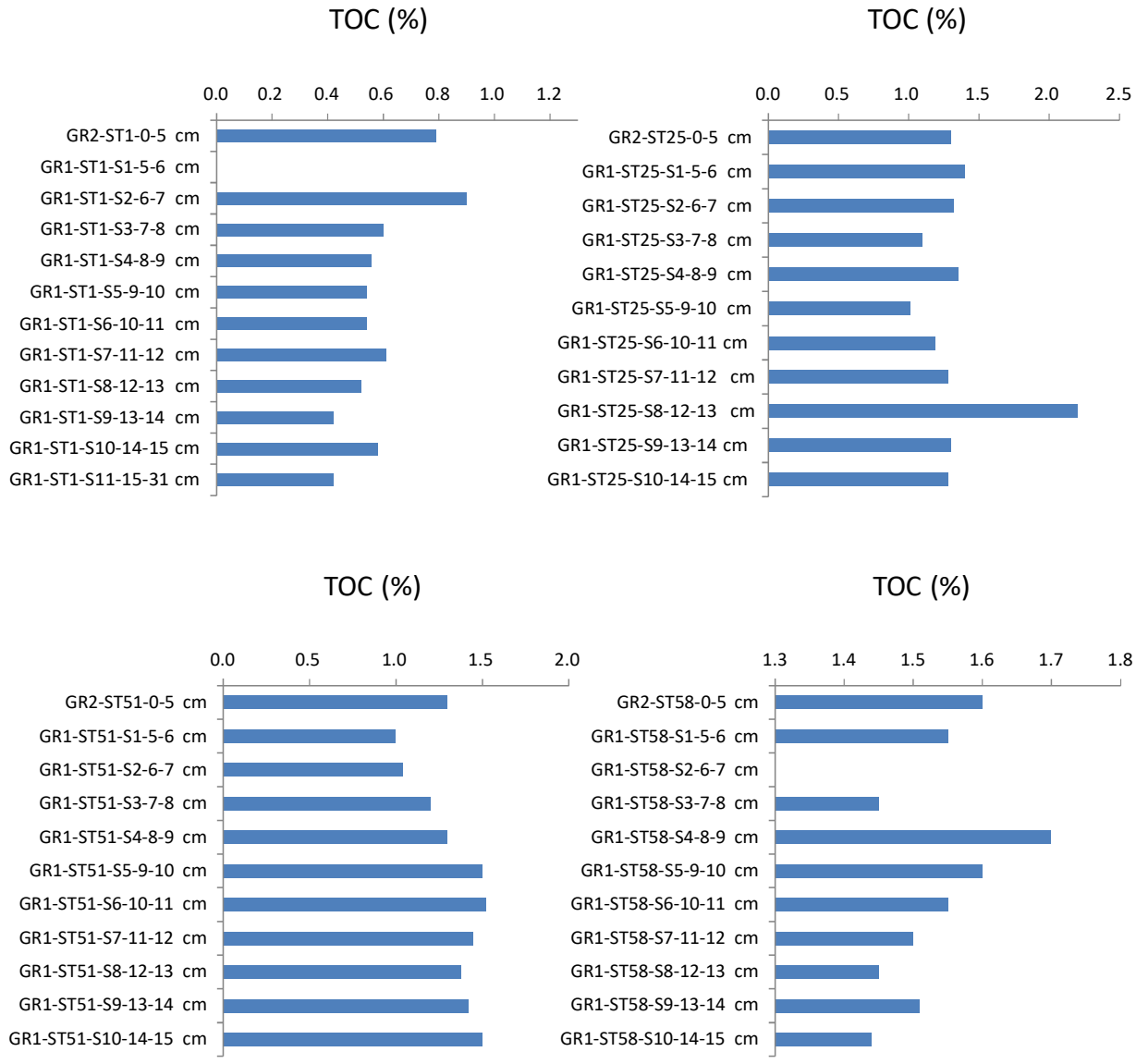

Figure 3. Total organic carbon (TOC) in different stations

According to the guidelines for pollution levels in the inner RSA bottom sediments (Massoud *et al*., 1996), concentrations of <15 µg g^{-1} as chrysene equivalent are considered to represent natural background levels in this Region. This threshold value was exceeded in the superficial sediment (GR-2) of station 25, and in particular in the S8 of this sediment core (GR1-ST-25- S8) with 627 µg g^{-1}; according to these guidelines, this section is heavily polluted, indicating

a high contamination by degraded crude oil. Further characterization and insights on the concentrations and sources of pollution on individual station are described below.

4.1. STATION 1

The vertical distribution of petroleum hydrocarbons are presented in the Figure 4. The highest concentration of petroleum hydrocarbons were measured in the sections 1 (GR1-ST1-S1-5-6 cm) and 10 (GR1-ST1-S1-14-15 cm) with concentration values of 35 µg g^{-1} (as ROPME equivalent). The GC-TPH concentration, as the sum of total aliphatic and total aromatic hydrocarbons measured by gas chromatography (GC) ranged from 19 to 100 µg g^{-1}. Whereas total hydrocarbon concentrations of >500 µg g^{-1} are generally indicative of a significant pollution, while values of <10 µg g^{-1} are considered to denote unpolluted sediments (Volkman *et al.*, 1992). Therefore, the TPH levels in sediment horizons reported here are relatively low compared to those in worldwide locations reported as chronically oil-contaminated, such as 60–646 µg g^{-1} in Hong Kong's Victoria Harbour (Hong *et al.*, 1995), 35-2900 µg g^{-1} in the New York Bight (Farrington & Tripp, 1977), and 11–6900 µg g^{-1} along the oil-impacted coastline of Saudi Arabia after the 1991 War (Readman *et al.*, 1996).

Figure 4. Total petroleum hydrocarbons as ROPME and GC equivalents from station 1

The aliphatic unresolved complex mixture (UCM) used as a relative measure of chronic/degraded oil contamination, hardly exceeded the background value of 10 µg g^{-1} in all sections, except for the superficial sample and sections 9 and 11. The UCM concentrations of <10 µg g^{-1} are comparable to coastal environments distant from hydrocarbon input, such as those in the eastern Mediterranean (Gogou *et al.*, 2000), the coastline of Ukraine in the Black Sea (Readman *et al.*, 2002) and in deep-basin sediments from the north-western Mediterranean Sea (Tolosa *et al.*, 1996).

The highest UCM value, up to 26 µg g^{-1}, was measured in S1, but low biodegradation of petroleum-related inputs was confirmed by the low ratio of UCM/*n*-alkanes (1.4–11) (Figure 5), and furthermore since values of >10 are indicative of chronic/degraded petroleum contamination (Simoneit, 1982). This low UCM centered at the carbon number *n*-C_{18}-*n*-C_{19}, indicated traces of some degraded diesel fuel.

Figure 5. Aliphatic UCM concentrations and UCM/n-alkanes diagnostic ratio from station 1

As shown in the Figure 6, most samples from the sediment core exhibited a dominance of the low even numbered carbon *n*-alkanes (*n*-C_{12} and *n*-C_{14}), derived probably from bacteria sources. In the top horizons of the core, this bacterial contribution was overlapped with the diesel fuel alkanes represented by the *n*-alkanes, from *n*-C_{15} to *n*-C_{20} with no odd/even predominance. The long-chain homologues (*n*-C_{27}, *n*-C_{29} and *n*-C_{31}) derived from terrestrial higher plant waxes were detected in all sections of the core. Concerning the source of the crude oil, the triterpane Tm/Ts ratio (3.1) from S1 approached the value of the Kuwait crude oil (Tm/Ts of 2.7) (Sauer *et al.*, 1993).

The PAHs in this station showed relatively low concentrations (144–586 ng g^{-1}) with the maximum value measured in S1. The total PAH concentrations in the core horizons given in the Figure 7, generally does mirror those found for the aliphatic UCM and TPH concentrations. The total PAH levels were >100 ng g^{-1} in all horizons of the samples and superficial sediment. Moderately contaminated sections, with PAHs values of > 100 ng g^{-1} but lower than 500 ng g^{-1} (Baumard *et al.*, 1998), included all horizons excepting for S1, which reached the maximum value of 586 ng g^{-1}. Nevertheless, these concentrations were lower than the NOAA sediment quality guideline value for the Effects Range Low (ERL) of 4000 ng g^{-1} dry weight (Long *et al.*, 1995).

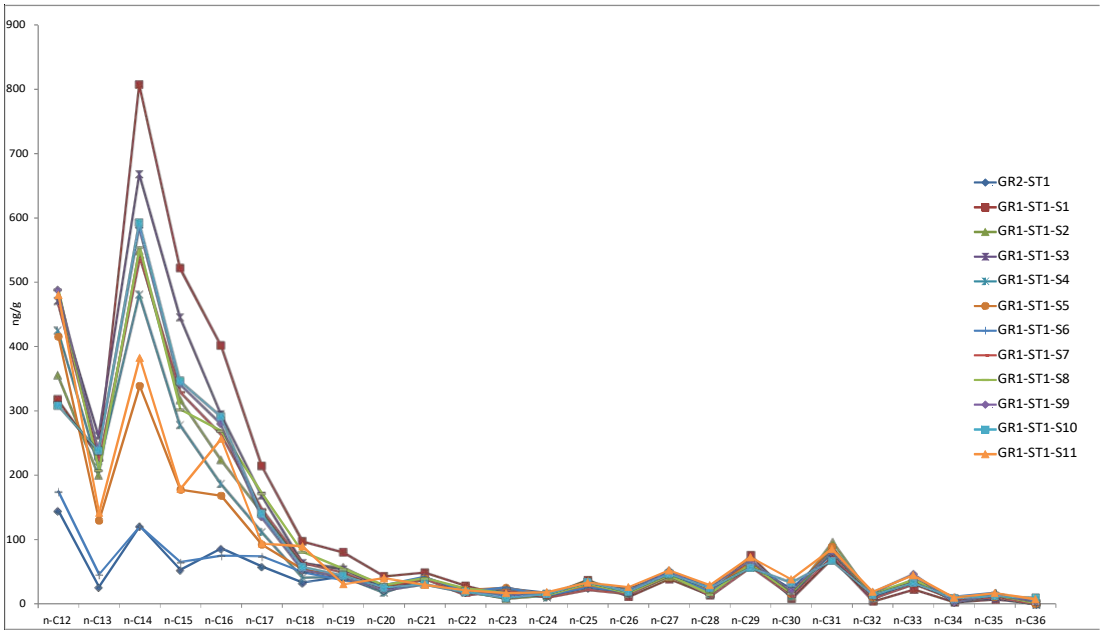

Figure 6. Distribution pattern of the n-alkanes in the different sections of the sediment core from station 1

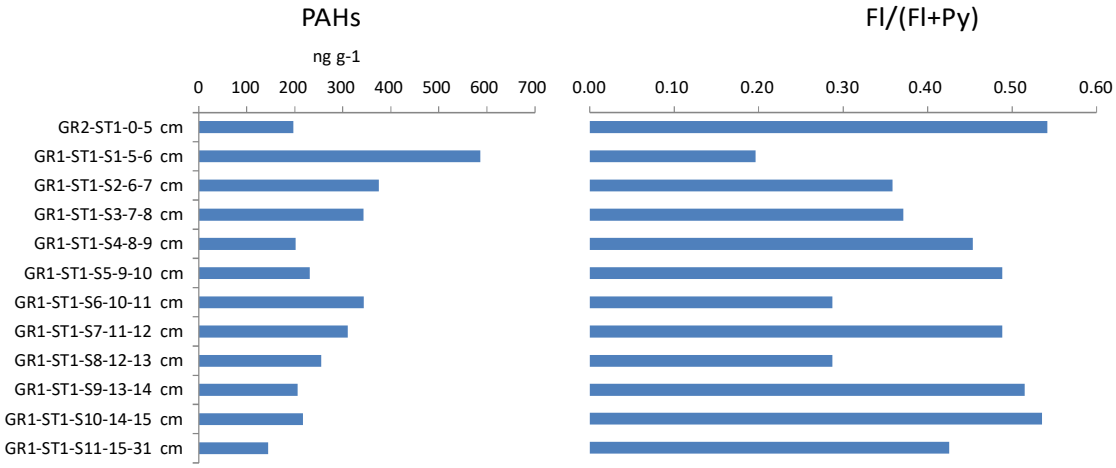

Figure 7. The total PAHs and Fl/(Fl+Py) ratio in the different sections of the sediment core from station 1

The representative PAH sedimentary patterns for selected sections are shown in the Figure 8 and tend to be similar down all the core's horizons. The PAHs were dominated by alkylated PAHs homologues of low molecular weight (2–3 rings PAHs) congeners, mainly alkylated phenanthrenes, dibenzothiophene, naphthalenes and fluorenes. The predominance of alkyl- substituted homologues over their respective parent compounds is a typical profile of oil- derived PAHs. No apparent pyrogenic PAHs sources featured by the dominance of the unsubstituted PAH over their alkylated homologues, and dominance of 4–6 rings PAH over the low molecular weight 2–3 rings PAH was observed. This is probably because the residual oil swamped out the

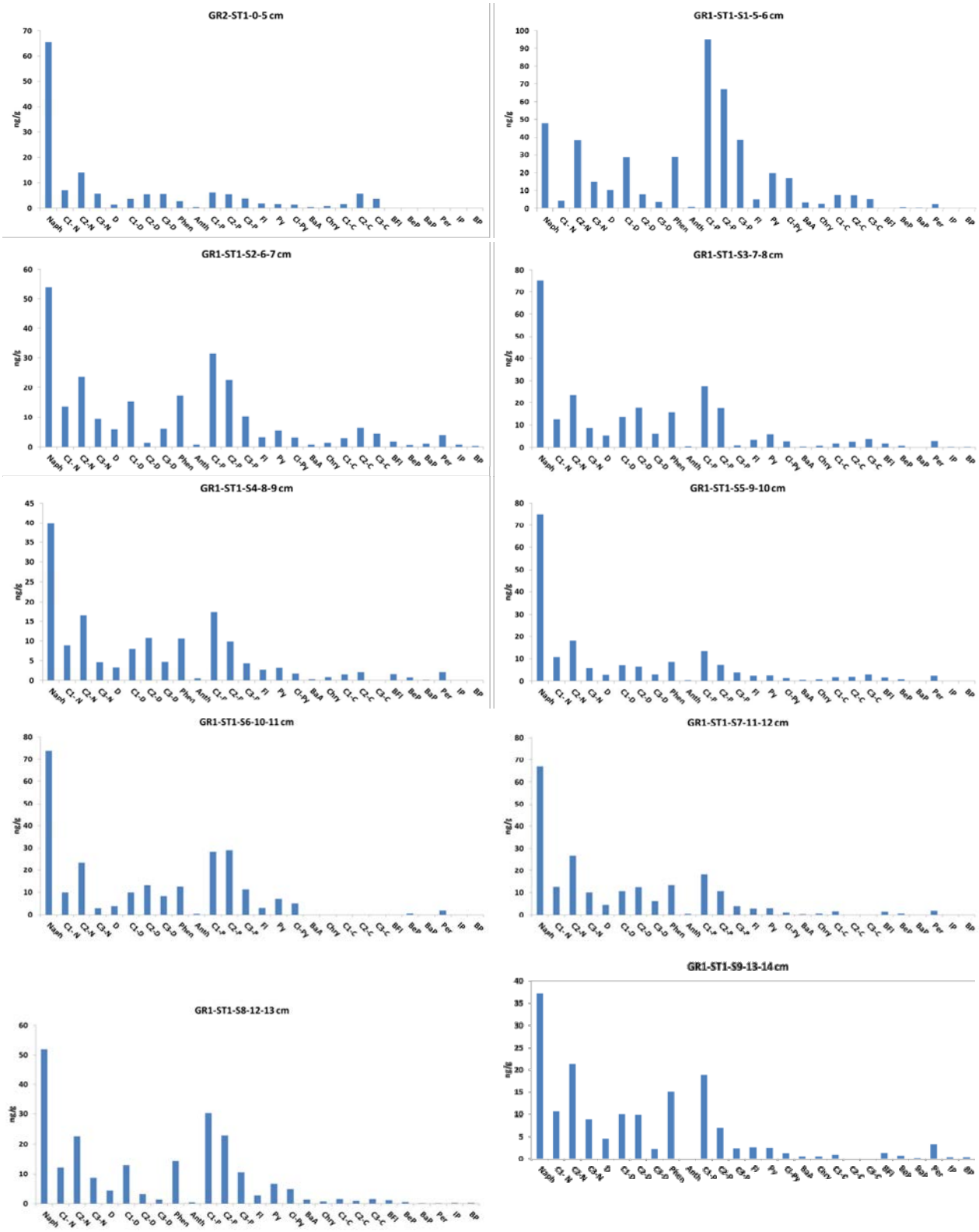

Figure 8. Distribution of selected PAHs in the core's horizons sediment samples from ST- 1. Compound codes: Naph: naphthalene; C1-, C2-, C3-N: mono-, di- and tri-methylnaphthalenes; D: dibenzothiophene; C1-, C2-, C3-D: mono-, di- and tri-methyldibenzothiophenes; Phen: phenanthrene; Anth: anthracene; C1-, C2-, C3-P: mono-, di- and tri-methylphenanthrenes; Fl: fluoranthene; Py: pyrene; C1-Py: mono-methyl pyrenes; BaA: benzo[a]anthracene; Chry: chrysene + triphenylene; C1-, C2-C, C3-C: mono-, di- and tri-methylchrysenes; BFl: benzo[b]fluoranthene + benzo[j]fluoranthene + benzo[k]fluoranthene + benzo[a]fluoranthene; BeP: benzo[e]pyrene; BaP: benzo[a]pyrene; Per: perylene; IB: indeno[1,2,3-cd]pyrene; BP: benzo[ghi]perylene.

low-level pyrogenic PAHs. The ratio of fluoranthene to pyrene Fl/(Fl+Py) (Figure 7) has been applied to assess the contribution of petroleum or combustion source of PAHs. A Fl/(Fl+Py) ratio greater than 0.5 has been used to indicate pyrogenic origins of PAHs (Baumard *et al.*, 1998) and <0.5 fossil derived sources. Here, the ratio Fl/(Fl+Py) showed some small changes through the core, but most of the values were lower than 0.5, suggesting that the PAHs in the sediment core were mainly derived from fuel oil pollution.

4.2. STATION 25

The vertical distribution of petroleum hydrocarbons in the station 25 are represented in the Figure 9. The TPH of this station showed relatively constant or low petroleum hydrocarbon concentrations throughout the core, excepting for the S8 (GR1-ST25-S8-12-13 cm) which peaked to concentration values of 5830 µg g^{-1} (as ROPME equivalent), and 480 µg g^{-1} as GC- TPH. This TPH levels are relatively high compare to those in worldwide locations reported as chronically oil-contaminated, such as 60-646 µg g^{-1} in Hong Kong's Victoria Harbour (Hong *et al.*, 1995). Nevertheless, they are in the lower range than those reported from the oil-impacted coastline of Saudi Arabia after the 1991 War of 11-6900 µg g^{-1} as GC-TPH (Readman *et al.*, 1996).

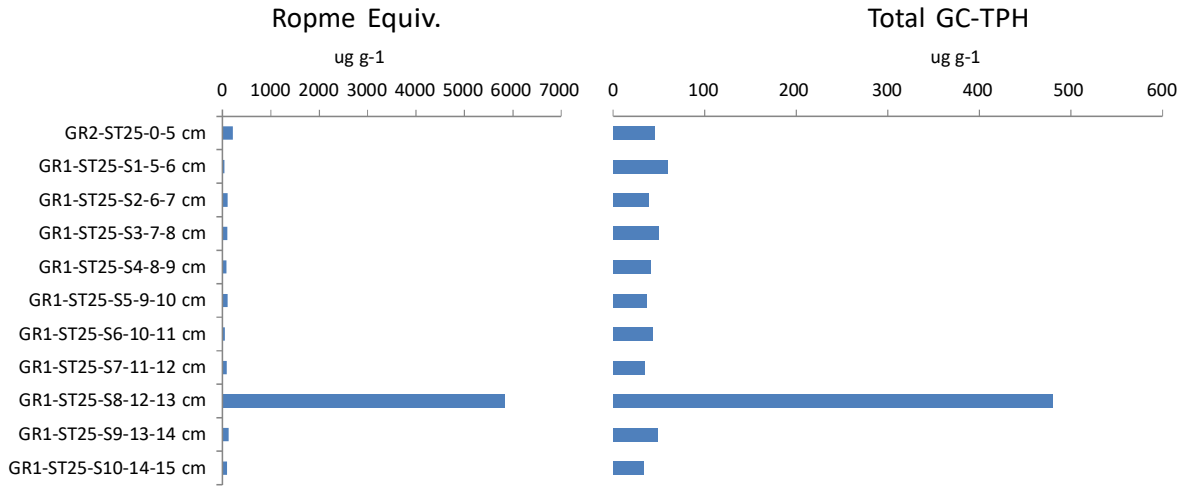

Figure 9. Total petroleum hydrocarbons as ROPME and GC equivalents from station 25

Excepting for the high contamination of the S8 horizon, the aliphatic UCM in the rest of the horizons rarely exceeded the value of 20 µg g^{-1}, evidencing a relatively low contamination by degraded oil. Only the most superficial section (S1) reached 27 µg g^{-1} but the low ratio of UCM/*n*-alkanes (<10) indicated a low biodegradation of petroleum-related inputs in this section (Figure 10). In contrast the S8, with a high UCM/*n*-alkanes ratio (96) confirmed the chronic/degraded petroleum contamination in

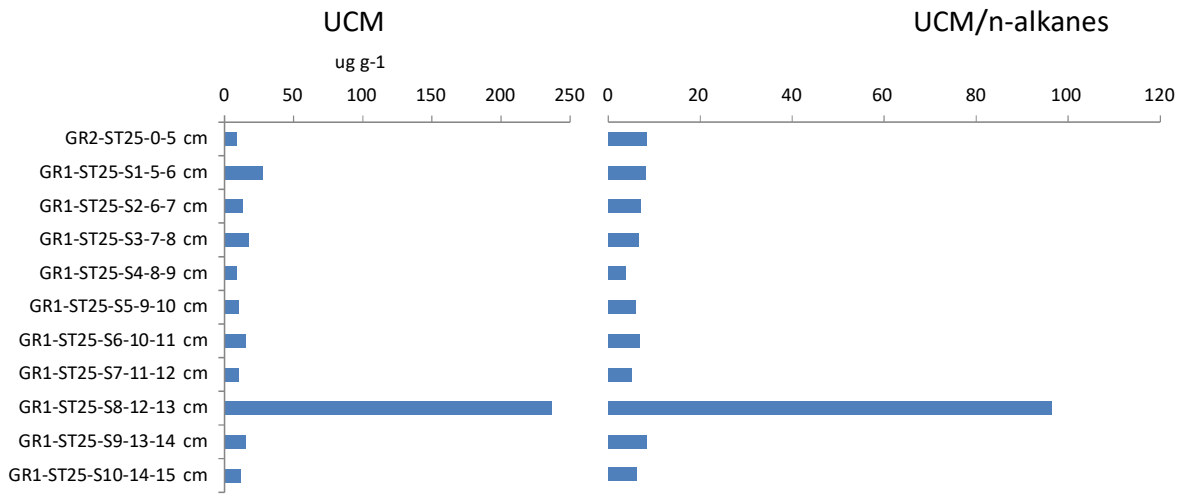

Figure 10. Aliphatic UCM concentrations and UCM/n-alkanes diagnostic ratio from station 25

this horizon (Simoneit, 1982). Moreover, their aliphatic GC profile was dominated by a bimodal unresolved complex mixture (UCM) centered at *n*-C_{22} and *n*-C_{29}, which infers to a pollution by light (diesel) and heavy petroleum fraction (heavy crude oil, Bunker C) having undergone weathering. For the other horizons, the poor UCM was only centered at the carbon number *n*-19, suggesting some input of diesel fuel weathered by time.

As shown in the Figure 11, most samples from the sediment core exhibited a dominance of the low even-numbered carbon *n*-alkanes (*n*-C_{12} and *n*-C_{14}) derived probably from bacteria sources. In the top horizons of the core, this bacterial contribution was overlapped with the diesel fuel alkanes.

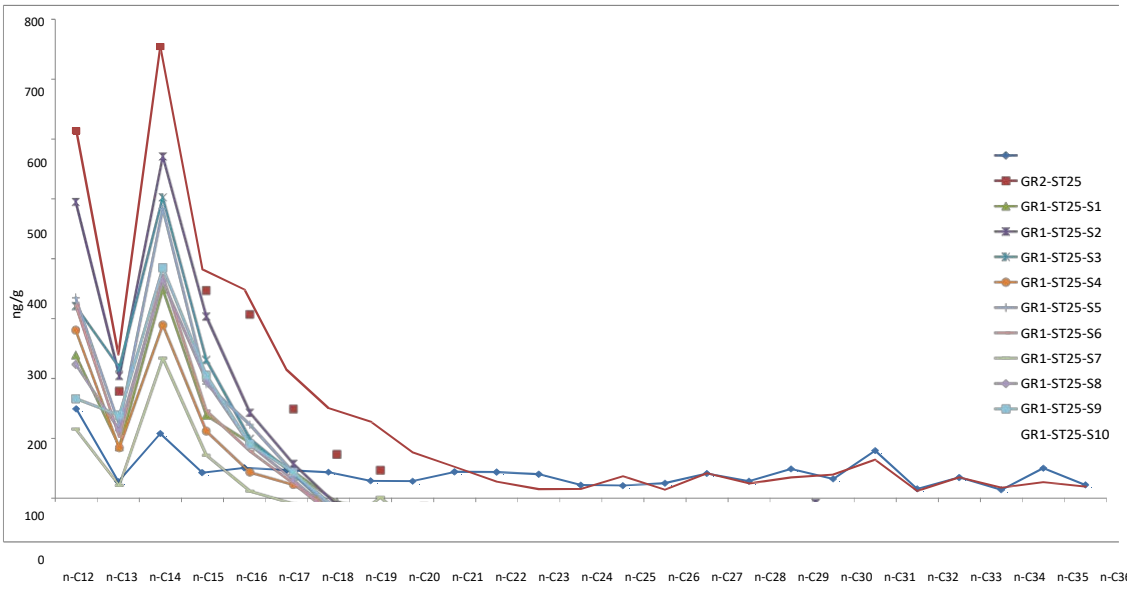

Figure 11. Distribution pattern of the n-alkanes in the different sections of the sediment core from station 25

Similarly to the station 1, the superficial sample of station 25 (GR2-ST25) showed only a small contribution of bacterial hydrocarbons in the low carbon range (*n*-C_{12} to *n*-C_{16}) and traces of fossil PAHs.

The total PAH concentrations in the core's horizons from station 25 are given in the Figure 12. Excepting for S8, the PAHs in this station showed relatively low concentrations (150–320 ng g^{-1}) and these values fell into the range considered to be moderately polluted (Baumard *et al.*, 1998). In contrast, the high PAHs concentrations values for S8 (2780 ng g^{-1}) indicate a heavily contaminated section. Fortunately, these concentrations were lower than the NOAA sediment quality guideline value for the Effects Range Low (ERL) of 4000 ng g^{-1} dry weight (Long *et al.*, 1995).

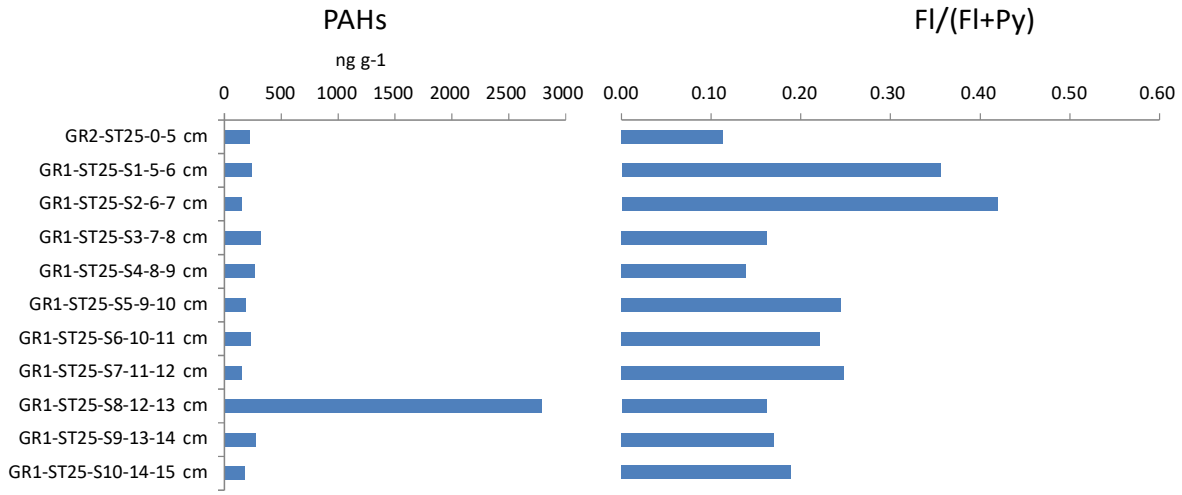

Figure 12. Total PAHs and Fl/(Fl+Py) ratio in the different sections of the sediment core from station 25

The representative PAH sedimentary patterns for selected sections are shown in the Figure 13 and tend to be similar to the station 1, and down all the core's horizons. Generally, the PAHs were dominated by alkylated PAHs homologues of low molecular weight (2–3 rings PAHs) congeners, mainly alkylated phenanthrenes, dibenzothiophene, naphthalenes and fluorenes typical of petrogenic sources. Only S8 exhibited a particular pattern with a high percentage of alkylated chrysenes and C3-dibenzothiophene, typical of a highly weathered oil source. Similarly to station 1, no apparent pyrogenic PAHs were observed. The ratio Fl/(Fl+Py) values (Figure 12) were much lower than 0.5, confirming that the PAHs in the sediment core were derived from fuel oil pollution. Concerning the source of the crude oil, the triterpane Tm/Ts ratio (3.1) from S8 approached the value of the Kuwait crude oil (Tm/Ts of 2.7) (Sauer *et al.*, 1993), whereas those from the upper core (S1) exhibited lower values (Tm/Ts of 2.4) which might indicate some mixture of Kuwait crude oil with a high Tm/Ts with the Light Arabian crude oil characterized by a low Tm/Ts value (0.88).

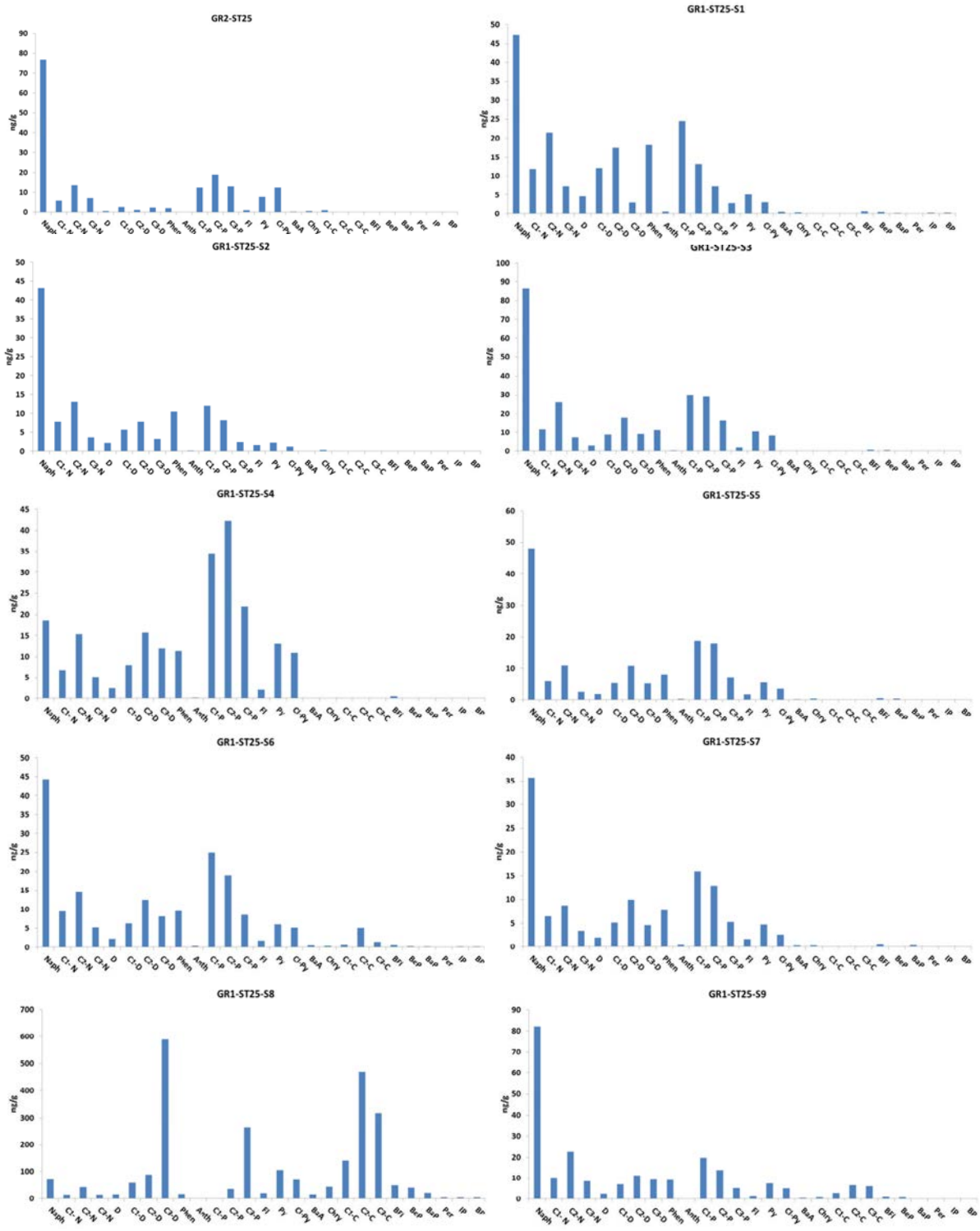

Figure 13. Distribution of selected PAHs in the core's horizons sediment samples from station 25. Compound codes are described in the Figure 8

4.3. STATION 51

The vertical distribution of petroleum hydrocarbons are presented in the Figure 14. The highest concentration of petroleum hydrocarbons as ROPME equivalent were measured in the superficial sample (GR2-ST51-0-5 cm) reaching the value of 120 µg g^{-1}. However, the total TPH concentrations measured by GC did not exhibit this maximum value in the surface sediment, and it showed fairly constant concentrations throughout the core (34–55 µg g^{-1}). These TPH levels are relatively low compared to those in worldwide locations reported as chronically oil-contaminated, such as 60–646 µg g^{-1} in Hong Kong's Victoria Harbour (Hong *et al.*, 1995), 35-2900 µg g^{-1} in the New York Bight (Farrington & Tripp, 1977), and 11-6900 µg g^{-1} along the oil-impacted coastline of Saudi Arabia after the 1991 War (Readman *et al.*, 1996).

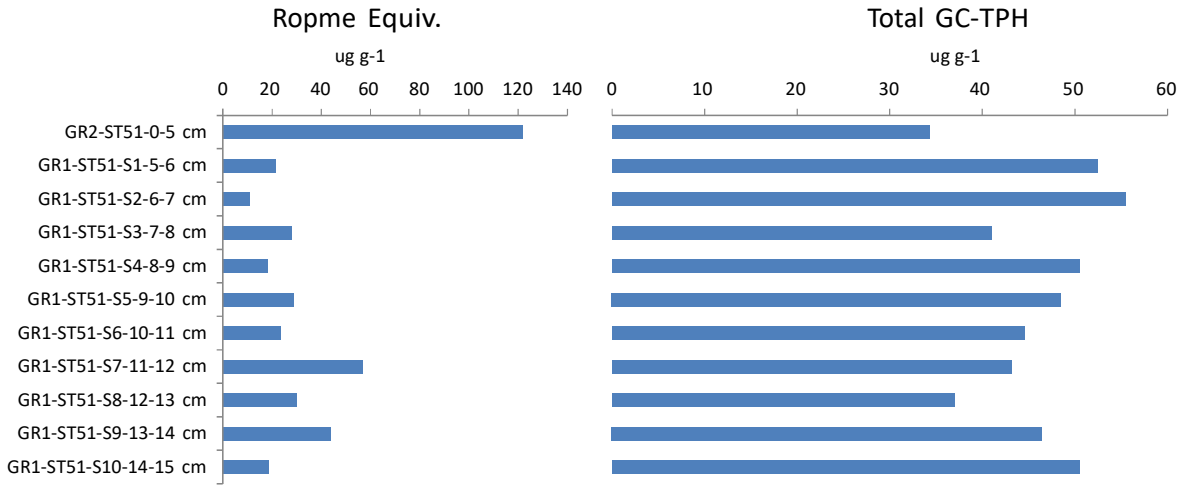

Figure 14. Total petroleum hydrocarbons as ROPME and GC equivalents from station 51

The aliphatic UCM concentrations ranged from 11 to 23 µg g^{-1} throughout the core with the highest values measured in S2 (Figure 15). The GC-profile of the UCM centered at the carbon number *n*-C_{18}-and *n*-C_{19}, indicates traces of degraded diesel fuel. However, the relatively low UCM concentrations together with the low ratios of UCM/*n*-alkanes (5–11) (Figure 15) reveal a low biodegradation of diesel oil (Simoneit, 1982).

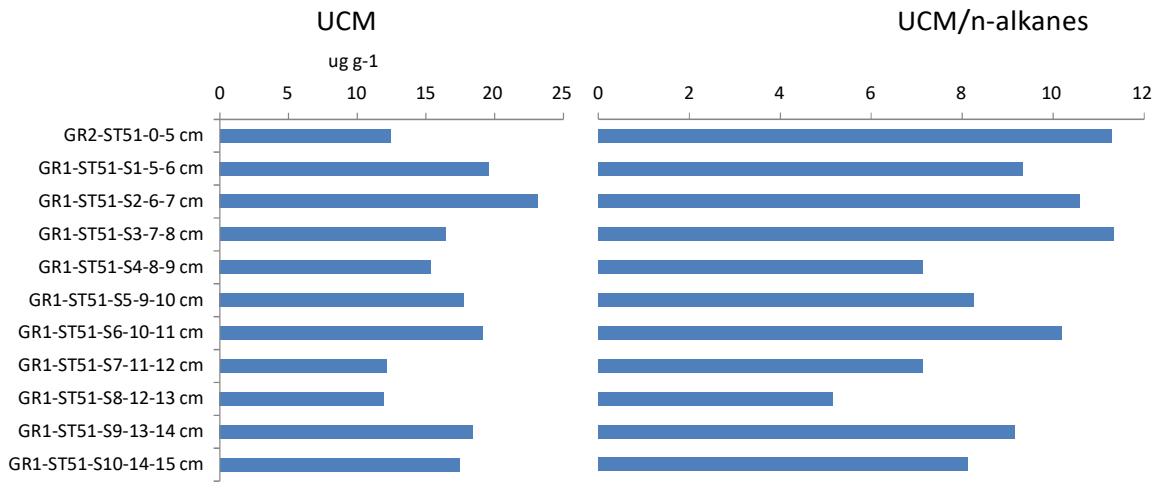

Figure 15. Aliphatic UCM concentrations and UCM/n-alkanes diagnostic ratio from station 51

As shown in the Figure 16, all sections from the core, exhibited the bacterial contribution of the low even carbon range *n*-alkanes (*n*-C_{12} and *n*-C_{14}) mixed with some diesel fuel (*n*-C_{15} to *n*-C_{20} alkanes with no odd/even predominance). The sections S1 and S2 exhibited also some contribution of heavy crude oil as evidenced by the range of *n*-alkanes, from *n*-C_{26} to *n*-C_{32} with no odd/even predominance. In contrast, the superficial sample taken in 2006 with the sediment grab, only exhibited bacterial hydrocarbons and traces of fresh oil pollution with no UCM.

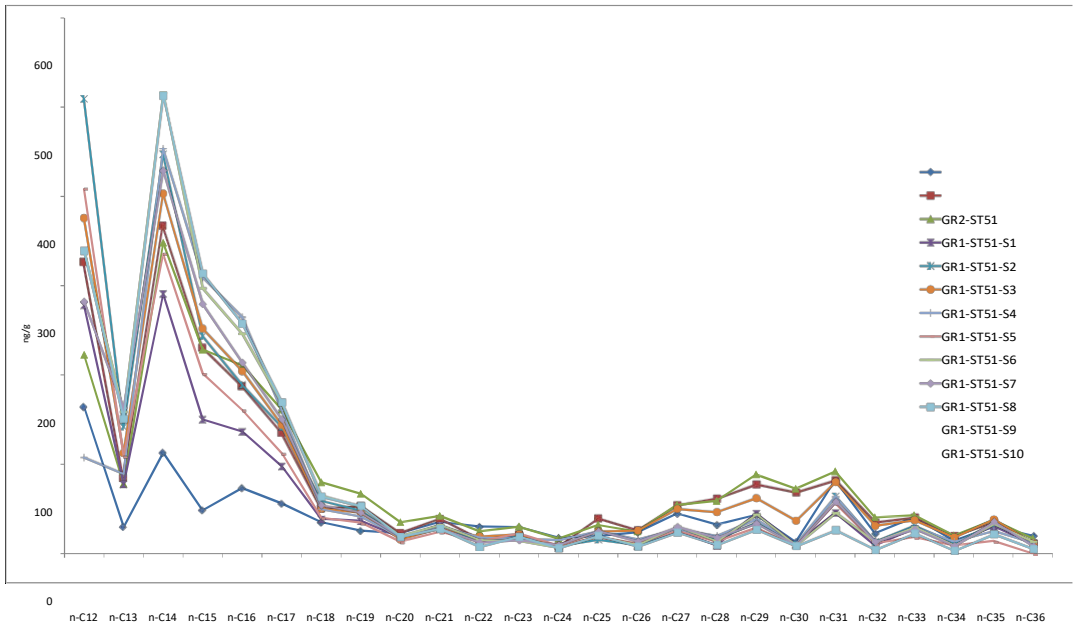

Figure 16. Distribution pattern of the n-alkanes in the different sections of the sediment core from station 51

The total PAH concentrations in the core's horizons from station 51 are given in the Figure 17. The PAHs in this station showed relatively low concentrations (106–323 ng g^{-1}), these values fell into the range considered to be moderately polluted (Baumard *et al*., 1998). Generally, the PAHs levels exceeding the value of 1 µg.g^{-1} are assigned to a chronically polluted area, where the PAHs are mainly derived from combustion/pyrolysis processes (Baumard *et al*., 1998).

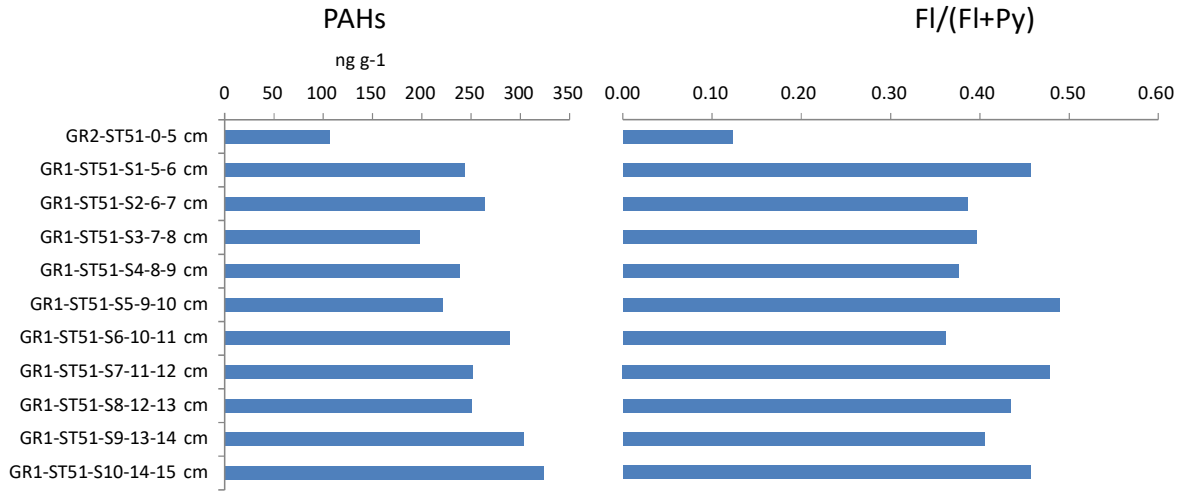

Figure 17. Total PAHs and Fl/(Fl+Py) ratio in the different sections of the sediment core from station 51

The representative PAH sedimentary patterns for selected sections are shown in the Figure 18 and tend to be similar to the stations 1 and 25; and down all the core's horizons where the distribution of PAHs dominated by alkylated PAHs homologues of phenanthrenes, dibenzothiophenes, naphthalenes and fluorenes are typical of petrogenic sources. Similarly to other stations, no apparent pyrogenic PAHs was observed, and the ratio Fl/(Fl+Py) values of <0.5 (Figure 17) confirm that most of the PAHs in the sediment cores were derived from fuel oil pollution. Concerning the source of the crude oil, the triterpane Tm/Ts ratio (0.99) from S2 approached the value of the Light Arabian crude oil (Tm/Ts of 0.88) (Sauer *et al*. 1993).

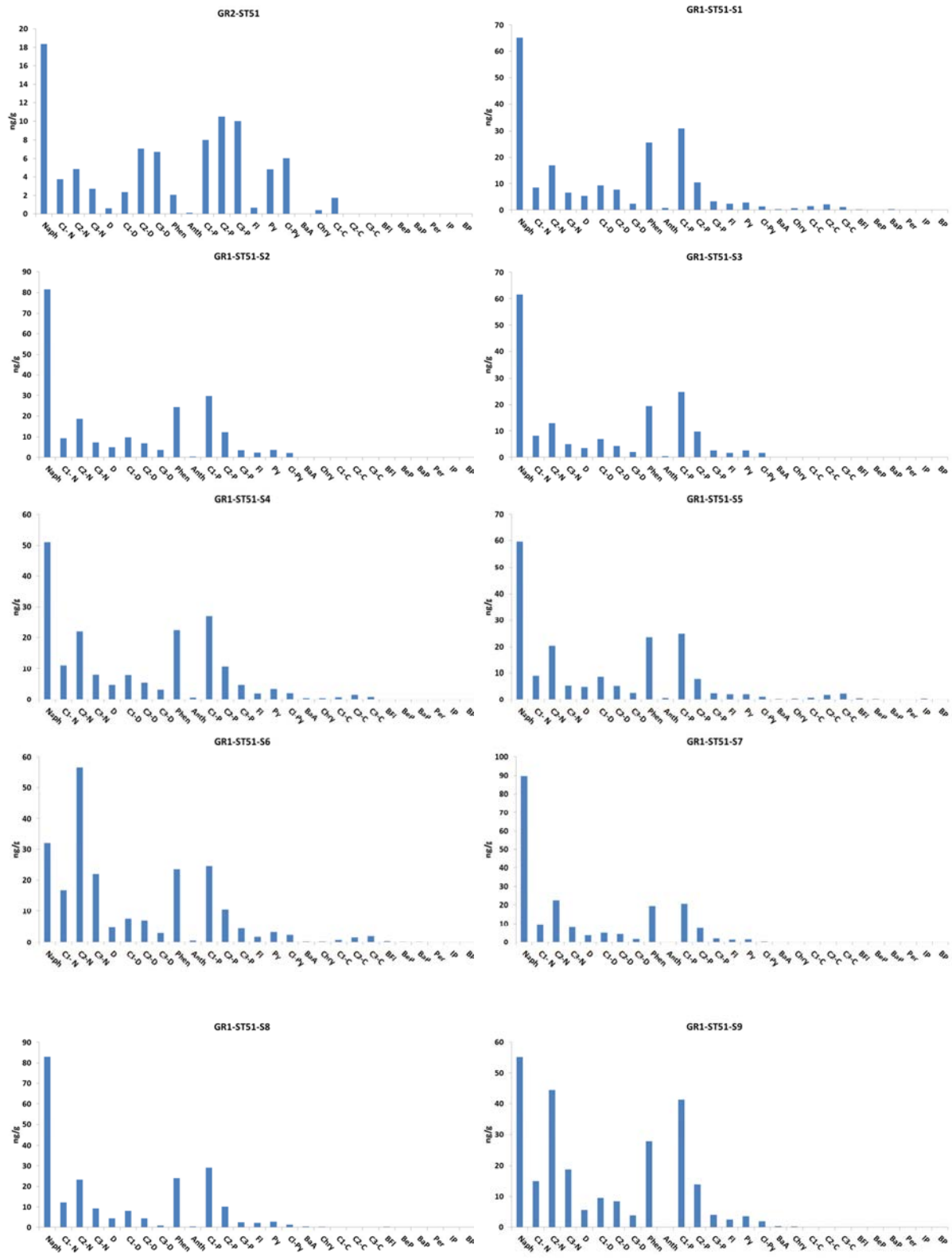

Figure 18. Distribution of selected PAHs in the core's horizons sediment samples from station 51. Compound codes are described in Figure 8

4.4. STATION 58

The vertical distribution of petroleum hydrocarbons are presented in the Figure 19. The total TPH concentrations throughout the core ranged from 26 to 81 µg g^{-1} as ROPME equivalent and from 34-192 µg g^{-1} as total GC-TPH. The highest concentrations of petroleum hydrocarbons were found in S4. The TPH levels in sediments reported here are moderately contaminated and they fell in the low range of locations reported as chronically oil- contaminated, such as 60–646 µg g-1 in Hong Kong's Victoria Harbour (Hong *et al.*, 1995), 35–2900 µg g-1 in the New York Bight (Farrington & Tripp, 1977), and 11–6900 µg g-1 along the oil-impacted coastline of Saudi Arabia after the 1991 War (Readman *et al.*, 1996).

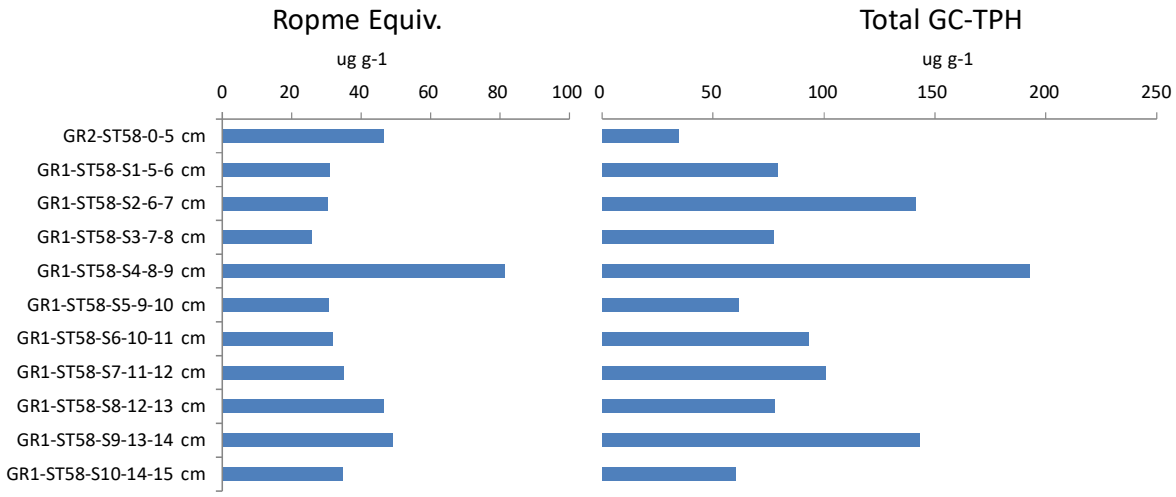

Figure 19. Total petroleum hydrocarbons as ROPME and GC equivalents from station 58

The aliphatic UCM concentrations through the core ranged from 8 to 115 µg g^{-1} and the peak concentrations occurred in the S4 and S9 horizon sections (Figure 20). Only these two sections with relatively high UCM concentrations and UCM/*n*-alkanes (33–45) showed substantial chronic degraded petroleum contamination (Simoneit, 1982). Except the superficial sample taken in 2006 by sediment grab, all the samples from the sediment core exhibited a similar profile typical of degraded light bunker oil with alkanes in the carbon range of *n*-C_{19} to *n*-$C_{25,}$ and a typical UCM "hump" centered at *n*-C_{22}. All samples including the superficial one showed also a distribution of even hydrocarbons in the low carbon number indicating a bacterial contribution.

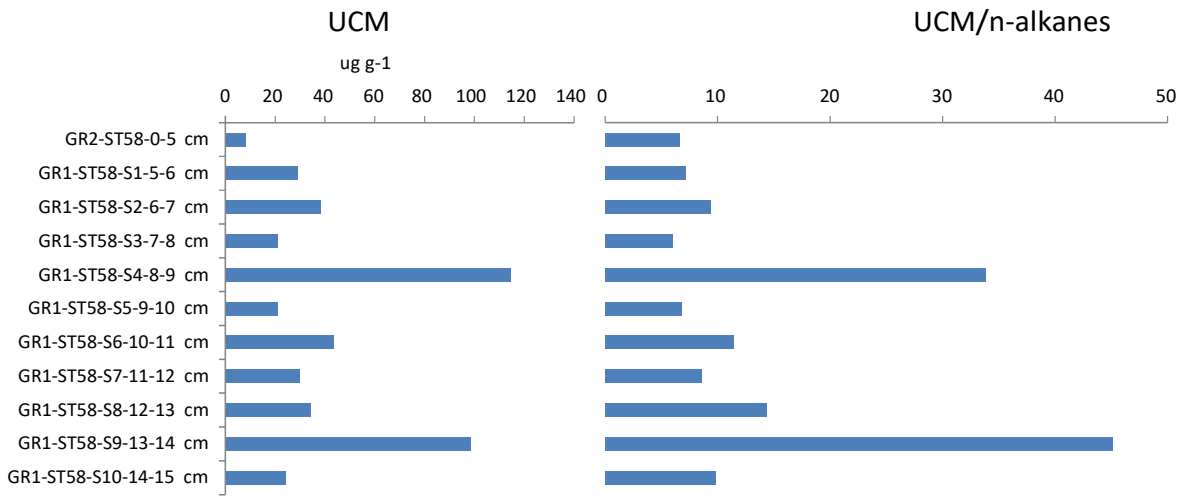

Figure 20. Aliphatic UCM concentrations and UCM/n-alkanes diagnostic ratio from station 58

The total PAH concentrations in the core's horizons from station 58 are given in the Figure 21. Except for the superficial sample that exhibited PAHs levels typical of low pollution (120 ng g^{-1}), the PAHs through the core sediment showed relatively high concentrations (510-2355 ng g^{-1}) and these values fell into the range considered to be chronically polluted (Baumard *et al.*, 1998). The maxima PAH concentrations were reached in S6, S4, S1 and S2.

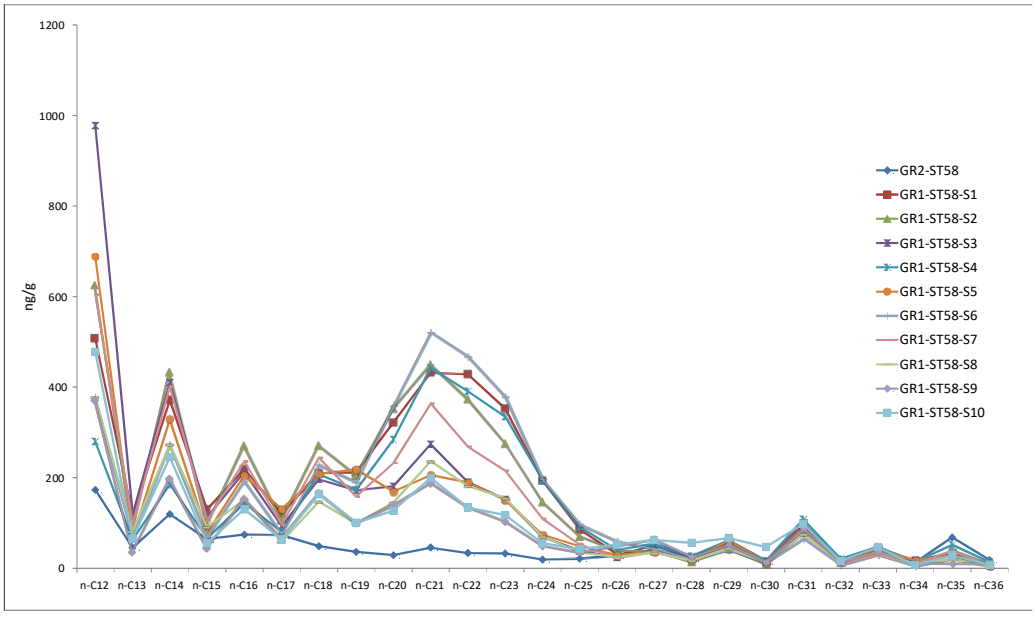

Figure 21. Distribution pattern of the n-alkanes in the different sections of the sediment core from station 58.

The composition of sedimentary PAHs did not show major variations through the core's horizons. The representative PAH sedimentary patterns for the different core horizons are shown in the Figure 23. A typical profile of petrogenic PAHs, with a predominance of alkyl- substituted phenanthrenes and alkylfluoranthene/pyrenes over their respective parent compounds, was observed. Some degree of physical weathering of the petrogenic profile was indicated by the loss of the more volatile PAHs, naphthalene, alkylnaphtalenes, fluorene, alkylfluorenes, dibenzothiophene and alkyldibenzothiophenes. Similarly to other stations, no apparent pyrogenic PAHs was observed, and the ratios Fl/(Fl+Py) (Figure 22) showed relatively constant values throughout the core (values < 0.1), confirming that most of the PAHs in the sediment core were derived from fuel oil pollution. Concerning the source of the crude oil, the triterpane Tm/Ts ratio (0.82) from S6 approached the value of the Light Arabian crude oil (Tm/Ts of 0.88) (Sauer *et al*., 1993).

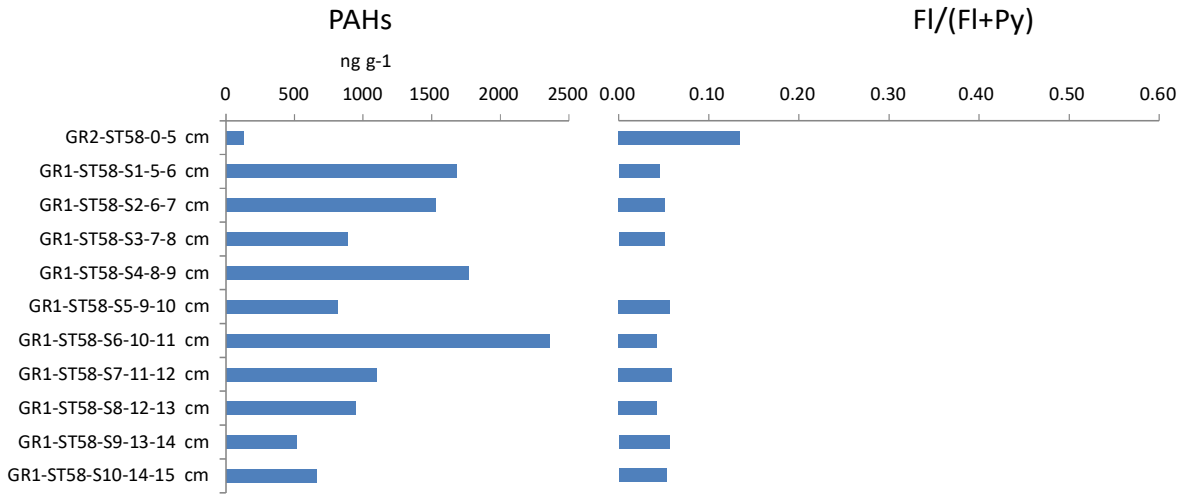

Figure 22. Total PAHs and Fl/(Fl+Py) ratio in the different sections of the sediment core from station 58

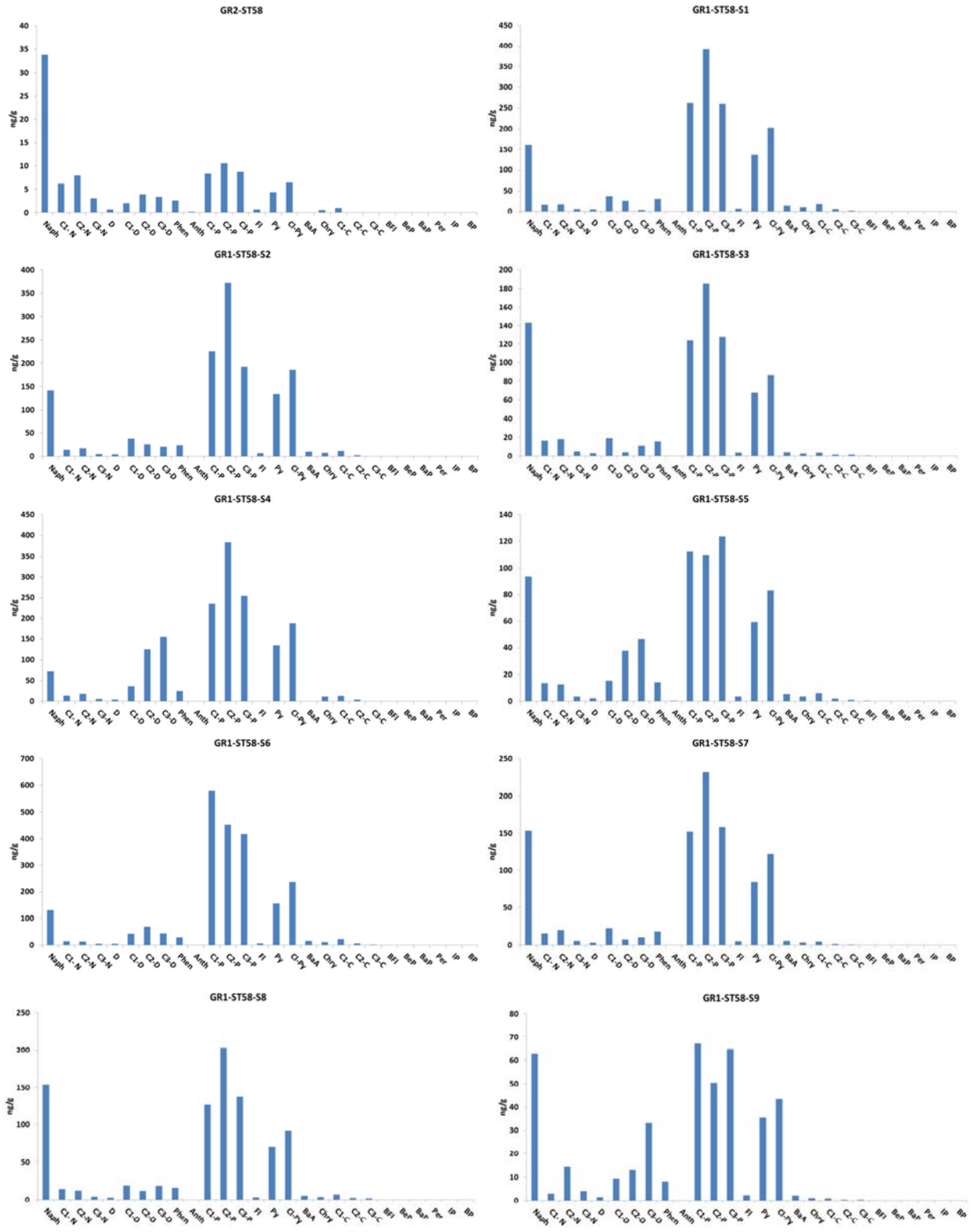

Figure 23. Distribution of selected PAHs in the core's horizons sediment samples from station 58. Compound codes are described in the Figure 8.

5. SUMMARY AND CONCLUSION

Among the 4 different sediment cores from the RSA, the superficial sediment of station 25 and in particular its S8 were heavily polluted, indicating a high contamination of degraded crude oil. By using diagnostic biomarkers ratios, the maximum concentration found at about 12–13 cm deep of station 25 was similar to the Kuwait reference crude oil which was spilled during the 1991 War. However, sediment dating would be needed to confirm this hypothesis. Moderately contaminated sections were also found in station 58, and in particular sections 4 and 9 showed substantial chronic contamination typical of degraded light bunker oil, with chemical diagnostic parameters similar to the Light Arabian crude oil. High concentrations of derived oil-PAHs were also found in the mid sections of station 58.

Interestingly, all of the other superficial samples did not exhibit important signs of oil pollution, since bacterial *n*-alkanes dominated over the small amounts of fossil PAHs. These substantial decreases in sedimentary levels of TPH and PAHs between 2001 and 2006, particularly in stations 1 and 58, which could be partially attributed to improvements in emission controls and to the continuous substitution of oil fuels by liquefied gases. The PAH distribution and concentration ratios were consistent with a petrogenic source of PAHs, and with a high proportion of alkylated PAHs. No apparent pyrogenic PAHs sources were observed, probably because the residual oil swamped out the low-level pyrogenic PAHs.

ACKNOWLEDGEMENTS

This was a collaborative project between the IAEA and ROPME, financially supported by both organizations. The Agency is grateful for the support provided to its Marine Environment Laboratory by the Government of the Principality of Monaco. We acknowledge with gratitude the help of Mr. Carlos Alonso and Beat Gasser for their carbon analysis.

For the purpose of the present work, the offshore sediment samples were provided from the ROPME Marine Sample Bank and the analyses were conducted by the Marine Environmental Studies Laboratory (MESL/IAEA) under a contract with ROPME.

REFERENCES

Baumard, P., Budzinski, H. & Garrigues, P. (1998). Polycyclic aromatic hydrocarbons in sediments and mussels of the western Mediterranean Sea. Environmental Toxicology and Chemistry, **17**, 765-776.

de Mora, S., Tolosa, I., Fowler, S.W., Villeneuve, J.-P., Cassi, R. & Cattini, C., (2010). Distribution of petroleum hydrocarbons and organochlorinated contaminants in marine biota and coastal sediments from the ROPME Sea Area during 2005. Marine Pollution Bulletin, **60**: 2323-2349.

Farrington, J.W. & Tripp, B.W., (1977). Hydrocarbons in western North Atlantic surface sediments. *Geochimica et Cosmochimica Acta,* **41**, 1627-1641.

Gogou, A., Bouloubassi, I. & Stephanou, E.G., (2000). Marine organic geochemistry of the Eastern Mediterranean: 1. Aliphatic and polyaromatic hydrocarbons in Cretan Sea surficial sediments. *Marine Chemistry*, **68**, 265-282.

Hong, H., L., X., L., Z., Chen, J.C., Wong, Y.S. & Wan, T.S.M., (1995). Environmental fate and chemistry of organic pollutants in the sediment of Xiamen harbor and Victoria harbor. *Marine Pollution Bulletin,* **31**, 229-236.

Long, E.R., MacDonald, D.D., Smith, S.L. & Calder, F.D., (1995). Incidence of adverse biological effects within ranges of chemical concentrations in marine and estuarine sediments. *Environmental Management,* **19**, 81-97.

Massoud, M.S., Al-Abdali, F., Al-Ghadban, A.N. & Al-Sarawi, M., (1996). Bottom sediments of the Gulf-II. TPH and TOC contents as indicators of oil pollution and implications for the effect and fate of the Kuwait oil slick. *Environmental Pollution,* **93**, 271-284.

Readman, J.W., Bartocci, J., Tolosa, I., Fowler, S.W., Oregioni, B. & Abdulraheem, M.Y., (1996). Recovery of the Coastal Marine Environment following the 1991 War- Related Oil Spills. *Marine Pollution Bulletin,* **32**, 493-498.

Readman, J.W., Fillmann, G., Tolosa, I., Bartocci, J., Villeneuve, J.-P., Catinni, C. & Mee, L.D., (2002). Petroleum and PAH contamination of the Black Sea. *Marine Pollution Bulletin,* **44**, 48-62.

Sauer, T., Brown, J.S., Boehm, P.D., Aurand, D.V., Michel, J. and Hayes, M.O., (1993). Hydrocarbon source identification and weathering characterization of intertidal and subtidal sediments along the Saudi Arabian coast after the 1991 War oil spill. *Marine Pollution Bulletin,* **27**, 117-134.

Simoneit, B.R.T. (1982). Some applications of computerized GC-MS to the determination of biogenic and anthropogenic organic matter in the environment. *Int. J. Environ. Anal. Chem.,* **12**, 177-193.

Tolosa, I., Bayona, J.M. & Albaiges, J., (1996). Aliphatic and Polycyclic Aromatic Hydrocarbons and Sulfur/Oxygen Derivatives in Northwestern Mediterranean Sediments: Spatial and Temporal variability, Fluxes, and Budgets. *Environmental Science and Technology,* **30**, 2495-2503.

Volkman, J.K., Holdsworth, D.G., Neill, G.P. & Bavor, J., H. J., (1992). Identification of natural, anthropogenic and petroleum hydrocarbons in aquatic sediments. *The Science of The Total Environment,* **112**, 203-219.

ANNEX - I

Table I.1. Concentration levels of Hydrocarbons, TOC and Diagnostic Ratios in Station 1

	TOC %	ROPME Equiv. ug g^{-1}	Chrysene Equiv. ug g^{-1}	Total GC-HCs ug g^{-1}	UCM ug g^{-1}	*n*-alkanes ug g^{-1}	UCM/*n*-alkanes	Total PAHs ng g^{-1}
GR2-ST1-0-5 cm	0.51	21	2.4	19.4	1.4	1.0	1.4	197.5
GR1-ST1-S1-5-6 cm	n.a	34	3.8	99.8	26.2	3.1	8.4	585.9
GR1-ST1-S2-6-7 cm	0.90	6.8	0.7	50.2	18.6	2.4	7.8	375.4
GR1-ST1-S3-7-8 cm	0.60	21	2.5	58.1	14.2	2.9	4.9	343.1
GR1-ST1-S4-8-9 cm	0.56	16	1.8	36.1	10.6	2.2	4.7	201.6
GR1-ST1-S5-9-10 cm	0.54	13	1.5	25.8	7.4	1.9	3.9	231.3
GR1-ST1-S6-10-11 cm	0.54	24	2.8	53.6	12.2	1.1	11.0	343.2
GR1-ST1-S7-11-12 cm	0.61	17	1.9	52.7	12.4	2.5	5.0	310.3
GR1-ST1-S8-12-13 cm	0.52	9	1.0	41.7	12.1	2.6	4.7	255.1
GR1-ST1-S9-13-14 cm	0.42	22	2.5	43.1	13.3	2.7	5.0	205.6
GR1-ST1-S10-14-15 cm	0.58	35	4.0	74.2	14.7	2.5	5.9	217.3
GR1-ST1-S11-15-31 cm	0.42	15	1.8	22.9	5.9	2.2	2.7	144.5

Table I.2. Concentration levels of Hydrocarbons, TOC and Diagnostic Ratios in Station 25

	TOC	**ROPME Equiv.**	**Chrysene Equiv.**	**Total GC-HCs**	**UCM**	***n*-alkanes**	**UCM/*n*-alkanes**	**Total PAHs**
	%	ug g^{-1}	ug g^{-1}	ug g^{-1}	ug g^{-1}	ug g^{-1}		ng g^{-1}
GR2-ST25-0-5 cm	0.85	213	24	45.4	9.2	1.1	8.5	226.4
GR1-ST25-S1-5-6 cm	1.40	39	4.3	60.0	27.6	3.4	8.1	238.6
GR1-ST25-S2-6-7 cm	1.32	105	12	39.3	13.0	1.8	7.1	151.2
GR1-ST25-S3-7-8 cm	1.10	99	11.0	49.7	17.4	2.6	6.7	319.9
GR1-ST25-S4-8-9 cm	1.35	79	8.9	41.0	8.7	2.2	3.9	266.5
GR1-ST25-S5-9-10 cm	1.01	108	12	37.3	10.5	1.7	6.0	188.4
GR1-ST25-S6-10-11 cm	1.19	46	5.1	43.0	15.2	2.2	7.0	231.6
GR1-ST25-S7-11-12 cm	1.28	87	9.8	34.4	10.2	2.0	5.2	156.4
GR1-ST25-S8-12-13 cm	2.20	5834	627	480.5	236.9	2.5	96.4	2786.0
GR1-ST25-S9-13-14 cm	1.30	124	14	48.7	15.4	1.8	8.4	274.7
GR1-ST25-S10-14-15 cm	1.28	92	10	32.9	11.9	1.9	6.2	184.4

Table I.3. Concentration levels of Hydrocarbons, TOC and Diagnostic Ratios in Station 51

	TOC	**ROPME Equiv.**	**Chrysene Equiv.**	**Total GC-HCs**	**UCM**	***n*-alkanes**	**UCM/*n*-alkanes**	**Total PAHs**
	%	ug g^{-1}	ug g^{-1}	ug g^{-1}	ug g^{-1}	ug g^{-1}		ng g^{-1}
GR2-ST51-0-5 cm	1.27	122	14	34.3	12.4	1.1	11.3	106.9
GR1-ST51-S1-5-6 cm	1.00	21	4.6	52.5	19.6	2.1	9.3	244.3
GR1-ST51-S2-6-7 cm	1.04	11	1	55.5	23.2	2.2	10.6	264.4
GR1-ST51-S3-7-8 cm	1.20	28	3.1	41.0	16.4	1.4	11.3	197.9
GR1-ST51-S4-8-9 cm	1.30	18	1.9	50.5	15.4	2.2	7.1	239.0
GR1-ST51-S5-9-10 cm	1.50	29	3	48.5	17.8	2.2	8.3	222.0
GR1-ST51-S6-10-11 cm	1.52	23	2.7	44.6	19.1	1.9	10.2	289.4
GR1-ST51-S7-11-12 cm	1.45	57	6.4	43.1	12.1	1.7	7.1	251.6
GR1-ST51-S8-12-13 cm	1.38	30	3.4	37.0	11.9	2.3	5.2	251.2
GR1-ST51-S9-13-14 cm	1.42	44	5	46.4	18.4	2.0	9.2	303.7
GR1-ST51-S10-14-15 cm	1.50	19	2	50.5	17.5	2.1	8.1	323.6

Table I.4. Concentration levels of Hydrocarbons, TOC and Diagnostic Ratios in Station 58

	TOC	**ROPME Equiv.**	**Chrysene Equiv.**	**Total GC-HCs**	**UCM**	***n*-alkanes**	**UCM/*n*-alkanes**	**Total PAHs**
	%	ug g^{-1}	ug g^{-1}	ug g^{-1}	ug g^{-1}	ug g^{-1}		ng g^{-1}
GR2-ST58-0-5 cm	1.38	47	5	34.3	8.1	1.2	6.6	127.8
GR1-ST58-S1-5-6 cm	1.55	31	3.5	79.2	29.2	4.1	7.1	1679.4
GR1-ST58-S2-6-7 cm	n.a	30	3.4	141.3	38.5	4.1	9.4	1526.2
GR1-ST58-S3-7-8 cm	1.45	26	2.9	77.1	21.2	3.5	6.0	889.8
GR1-ST58-S4-8-9 cm	1.70	81	9.1	192.9	114.7	3.4	33.8	1764.7
GR1-ST58-S5-9-10 cm	1.60	31	3.4	61.5	21.1	3.1	6.8	812.4
GR1-ST58-S6-10-11 cm	1.55	32	3.5	93.2	43.6	3.8	11.5	2354.5
GR1-ST58-S7-11-12 cm	1.50	35	3.9	100.9	30.0	3.5	8.6	1098.9
GR1-ST58-S8-12-13 cm	1.45	46	5	77.7	34.3	2.4	14.3	944.4
GR1-ST58-S9-13-14 cm	1.51	49	6	143.1	98.5	2.2	45.1	511.0
GR1-ST58-S10-14-15 cm	1.44	35	3.8	60.1	24.1	2.5	9.8	659.8

REGIONAL ORGANIZATION FOR THE PROTECTION OF THE MARINE ENVIRONMENT (ROPME)

P.O.BOX: 26388, SAFAT 13124, KUWAIT

Tel: (965)25312140 Fax: (965)25324172

Email : ropme@qualitynet.net